SHORT CONTRIBUTION

Negatively buoyant vertical jets

By TREVOR J. McDOUGALL *Research School of Earth Sciences, The Australian National University, P.O. Box 4, Canberra, 2600, A.C.T.*

1. Introduction

When a continuous jet of dense fluid is ejected vertically upwards into less dense surroundings it proceeds initially upwards, increasing in size and slowing down. The buoyancy force then becomes important, causing the plume to slow down even more and then, after reaching its maximum height, it falls down as an annular plume around the inner rising jet. This flow structure has been modelled both as a "double plume" (an inner rising circular forced plume and an outer sinking annular plume) on a computer and also in a laboratory experiment. This type of double plume structure has been invoked in the past to model the flow of dense salty water from the sea-bed (Turner and Gustafson (1978)), plumes driven by a source of bubbles in a stratified environment (McDougall (1978)) and cumulonimbus convection in the atmosphere (Berson and Baird (1975)). The evaluation of the buoyant body force for both the inner and the outer plumes has been very much an open question for these double plume structures and the main reason for doing this study was to compare the success of the two most reasonable body force formulations. The first formulation of the buoyant body force assumes that the constant-pressure surfaces are everywhere horizontal and this implies that the buoyant force acting on the inner plume is calculated by taking the density difference between the inner plume and the environment. The second formulation regards the outer plume as the "environment" for the inner plume and the density difference between these two plumes is used, together with the acceleration of the outer plume to evaluate the buoyant force for the inner plume. These two different methods of evaluating the buoyant body forces lead to two estimates of the height of rise of a negatively buoyant jet which differ by 20%.

2. The model

2.1 Conservation equations

The conservation equations of mass, momentum and buoyancy for a double plume structure have been derived by McDougall (1978) for the specific application of a bubble-plume in a stratified environment. Fig. 1 shows a sketch of a negatively buoyant jet which is injected vertically upwards from a small nozzle. In this paper we assume top-hat profiles of velocities and densities. The entrainment velocity into the inner plume from the outer plume is assumed to be $\alpha_\beta(v_1 + v_2)$, the entrainment velocity into the outer plume from the environment is assumed to be αv_2 and the entrainment velocity from the inner plume into the outer plume is assumed to be $\alpha_v v_2$ (see McDougall (1978), and Morton (1962) for further discussion on these entrainment assumptions). Taking z to be defined positive upwards and z^* positive downwards, the conservation of mass and buoyancy gives:

$$d(r_1^2 v_1)/dz = 2\alpha_\beta r_1(v_1 + v_2) - 2\alpha_v r_1 v_2 \qquad (1)$$

$$d([r_2^2 - r_1^2]v_2)/dz^* = -2\alpha_\beta r_1(v_1 + v_2) + 2\alpha_v r_1 v_2$$
$$+ 2\alpha r_2 v_2, \qquad (2)$$

$$d(r_1^2 v_1 g_1')/dz = 2\alpha_\beta r_1(v_1 + v_2)g_2' - 2\alpha_v r_1 v_2 g_1' \qquad (3)$$

and

$$d([r_2^2 - r_1^2]v_2 g_2')/dz^* = -2\alpha_\beta r_1(v_1 + v_2)g_2'$$
$$+ 2\alpha_v r_1 v_2 g_1' \qquad (4)$$
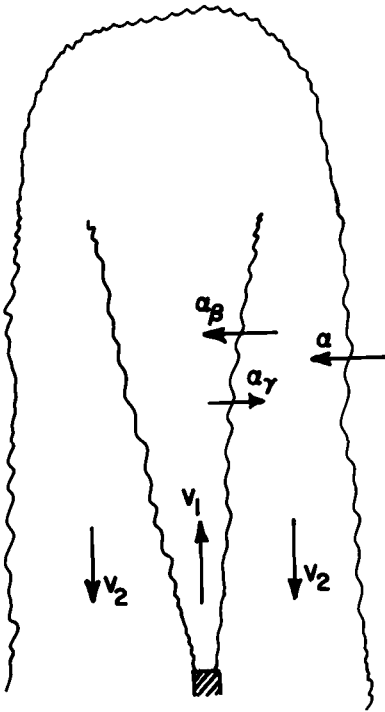
Fig. 1. Sketch showing the upward-moving inner circular plume surrounded by the downward-moving outer annular plume. The three entrainment processes are parameterized by the three entrainment coefficients α_β, α_γ and α.

where

$$g_1' = g(\rho_1 - \rho_0)/\rho_0, \, g_2' = g(\rho_2 - \rho_0)/\rho_0, \, \rho_0$$

is the (uniform) density of the environment and r_1 and r_2 are the radii of the inner and the outer plumes respectively.

The first formulation of the buoyant body forces assumes that constant pressure surfaces remain horizontal through the environment and both plumes. This leads to the following vertical momentum equations,

$$d(r_1^2 v_1^2)/dz = -r_1^2 g_1' - 2\alpha_\beta r_1 v_2(v_1 + v_2)$$
$$- 2\alpha_\gamma r_1 v_1 v_2, \tag{5}$$

and

$$d([r_2^2 - r_1^2]v_2^2)/dz^* = [r_2^2 - r_1^2]g_2'$$
$$- 2\alpha_\beta r_1 v_2(v_1 + v_2) - 2\alpha_\gamma r_1 v_1 v_2. \tag{6}$$

The second method of evaluating the buoyant body force on the inner plume refers the density of the inner plume to the density of the outer plume

instead of to the environment. In this way, the outer plume is regarded as the "environment" for the inner plume and so we must also include the acceleration of this frame of reference (see McDougall, 1978). This second method of evaluating the buoyant forces on the inner plume leads to

$$d(r_1^2 v_1^2)/dz = -r_1^2(g_1' - g_2' + v_2\, dv_2/dz^*)$$
$$- 2\alpha_\beta r_1 v_2(v_1 + v_2)$$
$$- 2\alpha_\gamma r_1 v_1 v_2. \tag{7}$$

We further assume that in taking the momentum equation across both plumes together, we can evaluate the total buoyant body force with respect to the density of the environment, i.e.

$$d(r_1^2 v_1^2)/dz - d([r_2^2 - r_1^2]v_2^2)/dz^* = -r_1^2 g_1'$$
$$- [r_2^2 - r_1^2]g_2'. \tag{8}$$

Equations (7) and (8) give

$$d([r_2^2 - r_1^2]v_2^2)/dz^* = [r_2^2 - r_1^2]g_2' + r_1^2(g_2'$$
$$- v_2\, dv_2/dz^*) - 2\alpha_\beta r_1 v_2(v_1 + v_2) - 2\alpha_\gamma r_1 v_1 v_2. \tag{9}$$

The acceleration of the outer plume, $v_2\, dv_2/dz^*$ in these equations can be readily calculated from (2) and (9).

2.1.1 *Nondimensional variables*

There are two dimensional variables which characterize a negatively buoyant vertical jet, firstly the buoyancy flux $\rho_0 F_0$ and secondly the momentum flux $\rho_0 M_0$ from the source. The influence of the mass flux from the source is assumed negligible (Morton (1959)). The nondimensional variables, x, x^*, R_1, R_2, S, V_1, V_2, G_1 and G_2 are defined by

$$z = M_0^{3/4} F_0^{-1/2} x,$$
$$z^* = M_0^{3/4} F_0^{-1/2} x^*,$$
$$r_1 = \alpha M_0^{3/4} F_0^{-1/2} R_1, \qquad r_2 = \alpha M_0^{3/4} F_0^{-1/2} R_2,$$
$$v_1 = M_0^{-1/4} F_0^{1/2} V_1, \qquad v_2 = M_0^{-1/4} F_0^{1/2} V_2,$$
$$g_1' = M_0^{-5/4} F_0^{3/2} G_1, \qquad g_2' = M_0^{-5/4} F_0^{3/2} G_2,$$

and $S^2 = R_2^2 - R_1^2$.

With these variables, the differential equations become

$$d(R_1^2 V_1)/dx = 2\beta R_1(V_1 + V_2) - 2\gamma R_1 V_2, \tag{10}$$
$$d(S^2 V_2)/dx^* = -2\beta R_1(V_1 + V_2) + 2\gamma R_1 V_2$$
$$+ 2R_2 V_2, \tag{11}$$

$$d(R_1^2 V_1 G_1)/dx = 2\beta R_1(V_1 + V_2)G_2 - 2\gamma R_1 V_2 G_1,$$
(12)

$$d(S^2 V_2 G_2)/dx^* = -2\beta R_1(V_1 + V_2)G_2$$
$$+ 2\gamma R_1 V_2 G_1,$$
(13)

and for the first method of buoyant force evaluation

$$d(R_1^2 V_1^2)/dx = -R_1^2 G_1 - 2\beta R_1 V_2(V_1 + V_2)$$
$$- 2\gamma R_1 V_1 V_2,$$
(14)

$$d(S^2 V_2^2)/dx^* = S^2 G_2 - 2\beta R_1 V_2(V_1 + V_2)$$
$$- 2\gamma R_1 V_1 V_2,$$
(15)

while for the second method of buoyant force evaluation we have

$$d(R_1^2 V_1^2)/dx = -R_1^2(G_1 - G_2 + V_2 dV_2/dx^*)$$
$$- 2\beta R_1 V_2(V_1 + V_2) - 2\gamma R_1 V_1 V_2$$
(16)

and

$$d(S^2 V_2^2)/dx^* = S^2 G_2 + R_1^2(G_2 - V_2 dV_2/dx^*)$$
$$- 2\beta R_1 V_2(V_1 + V_2) - 2\gamma R_1 V_1 V_2.$$
(17)

Here we have put $\beta = \alpha_\beta/\alpha$ and $\gamma = \alpha_v/\alpha$.

2.2 Starting conditions for the jet

Near the nozzle the upward-moving inner jet is virtually unaffected by its negative buoyancy and it behaves like a pure jet (see Morton (1959)). Setting $z = 0$ at the virtual origin of the jet, the radius at a small height z_s is given by $r_1 = 2\alpha_\beta z_s$ (Turner (1973) page 172) or, $R_1 = 2\beta x_s$. In the computer programme the starting value of x was $x_s = 0.05$. The upwards momentum flux at the nozzle is defined by $\rho_0 M_0 = \pi \rho_0 r_1^2 v_1^2$ and this leads to a starting value of V_1 equal to $(2\pi^{1/2} \beta \alpha x_s)^{-1}$. The flux of buoyancy at the nozzle defined by $\rho_0 F_0 = \pi \rho_0 r_1^2 v_1/g_1'$ and this gives $G_1 = V_1$ at the starting value of x_s.

2.3 Method of the computer solutions

The three differential eqs. (10), (12) and either (14) or (16) which describe the variation of the mass flux, the buoyancy flux and the momentum flux of the inner plume are integrated numerically from the starting condition at $x_s = 0.05$ up to a height at which the inner plume has slowed down considerably and is about to stop its upwards ascent and begin to fall downwards. For the first integration up the inner plume we take $V_2 = S^2 =$

0, that is, we ignore the presence of the outer plume. Having reached the end of the inner plume integration, we then integrate the three differential equations of the outer plume downwards until we arrive at the starting value of x (=x_s) again. During this downward integration the values used for R_1, V_1 and G_1 at each level are those derived by the previous integration up the inner plume. This process of integrating up the inner plume and down the outer plume is performed many times until a steady state is achieved.

The upward integration is stopped at $x = x_f$ when the velocity of the inner plume has fallen below $(2g_1' r_1)^{1/2}$. This condition is equivalent to $V_1^2 \leq 2\alpha R_1 G_1$.

When the solution is steady, the downward flux of buoyancy in the outer plume at x_s is equal to $\rho_0 F_0$, that is $\pi \alpha^2 S^2 V_2 G_2 = 1$ at x_s. This condition was used as a test of whether the solution had reached a steady state. $\pi \alpha^2 S^2 V_2 G_2 - 1$ was usually about ± 0.02 after 10 iterations. The results presented in this paper were all after 20 iterations by which stage $|\pi \alpha^2 S^2 V_2 G_2 - 1|$ was less than 0.005.

2.4 Treatment of the region where the plume turns around.

When the upward integration finishes at x_f the fluid of the inner plume continues to rise a little above this level while at the same time turning around, spreading out a little and then beginning to sink as an annular plume. If we assume that in this region there is no appreciable mixing with the surroundings and that the flow is steady, we have at this level

$$G_2 = G_1$$
(18)

and

$$S^2 V_2 = R_1^2 V_1.$$
(19)

Fig. 2 shows a sketch of this region of the flow. We have assumed here a shape which is a cylinder of height h capped by a hemisphere of radius r_2. The application of the vertical momentum equation to the control volume which is defined as this cylindrical and hemispherical shape gives

$$(\pi r_2^2 h + 2/3\pi r_2^3)g_1' = \pi(r_2^2 - r_1^2)v_2^2 + \pi r_1^2 v_1^2$$
(20)

where the left hand side is the downward force on the fluid in this control volume and the right hand side of (20) is equal to the flux of downward
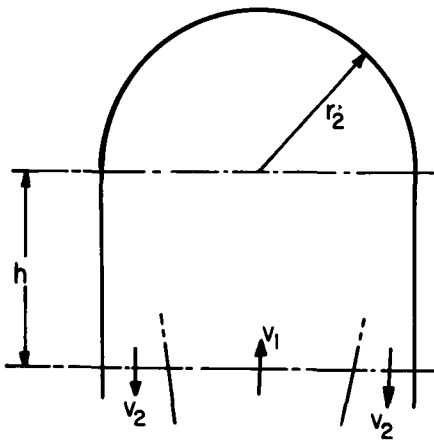
Fig. 2. Sketch of the region where the jet turns around.

momentum out of the control volume. This equation is equivalent to

$$1/3\left[\left(\frac{R_2}{R_1}\right)^2 - 1\right]\left[\frac{R_2}{R_1}\right]\left[\frac{2\alpha R_1 G}{V_1^2}\right]\left[3/2\,\frac{h}{r_2} + 1\right]$$
$$- 1 = 0, \tag{21}$$

and for any given value of h/r_2 this equation is solved by Newton's method to give R_2/R_1. In this way the assumed size of the cap (i.e. h/r_2) leads to R_2 and hence V_2 (from (19)) at x_f which are needed as the initial values for the integration down the outer plume. The total height of rise of the jet is given by

$$x_{max} = x_f + \alpha R_2\left(\frac{h}{r_2} + 1\right). \tag{22}$$

3. Results of the model

The most fundamental characteristic of a negatively buoyant vertical jet is its height of rise. Turner (1966) performed a series of experiments with dense salty jets injected upwards. He measured the volume flow rate of the jet fluid, the initial buoyancy g_1' and the radius of the jet. He calculated the momentum flux using the measured volume flow rate and the nozzle radius and found that $z_{max} = 1.85\,M_0^{3/4}\,F_0^{-1/2}$. However the flow out of the nozzle at the laboratory Reynolds numbers is likely to be close to a Poiseuille flow rather than having a constant velocity (mean velocity $= u_m$)

across the nozzle and this has a significant effect on the momentum flux, as we show below. The velocity at radius r of a Poiseuille flow in a tube of radius a is $u(r) = 2u_m(1 - r^2/a^2)$. The integrated mass flux across the nozzle is then $\pi\rho_0 a^2 u_m$ and the integrated momentum flux is $4/3\pi\rho_0 a^2 u_m^2$. This means that the actual momentum flux, $\rho_0 M_0$ is 4/3 of that used by Turner which was based on the mean velocity across the nozzle. Therefore, in terms of the true momentum and buoyancy fluxes from the source, the maximum height of rise found from experiment is

$$z_{max} = 1.5\,M_0^{3/4}\,F_0^{-1/2}. \tag{23}$$

We performed several laboratory experiments with dense salty jets forced upwards. The jet fluid contained many very small polythene spheres and we obtained streak photographs of the double plume structure with side slit-lighting against a black background. These experiments confirmed that $z_{max} = 1.5\,M_0^{3/4}\,F_0^{-1/2}$ (where M_0 is calculated by assuming a Poiseuille velocity profile at the nozzle) and the included angle of the inner plume was consistent with $\alpha_\beta = 0.056$.

Fig. 3 shows the results of the model with the second formulation of the buoyant body forces for $\alpha = 0.085$, $\gamma = 1.0$, $\alpha_\beta = 0.056$ and $h/r_2 = 2$. We will consider the effects of variations in these four parameters before we study the consequences of the two different buoyant force formulations. The values of α and α_β are taken from List and Imberger (1973) as being the values of the entrainment coefficients appropriate to a pure plume and a pure jet respectively. Because the inner plume initially behaves like a pure jet, it seems reasonable to choose $\alpha_\beta = 0.056$, however this value could perhaps be varied in the upper half of the flow where the buoyancy of the inner plume begins to dominate its momentum. While the downward-flowing outer plume is driven by buoyancy and so a value of α equal to 0.085 (which is appropriate to a pure plume) seems reasonable, the flow here is different to a normal plume because the eddies do not extend across the whole width of the double plume structure. For this reason we show results in Fig. 4 for a different value of α, namely $\alpha = 0.10$. The profile of the outer radius r_2 of the double plume structure looks more believable with $\alpha = 0.10$ as this avoids the "necking in" which is apparent near the top of the outer plume with $\alpha = 0.085$.
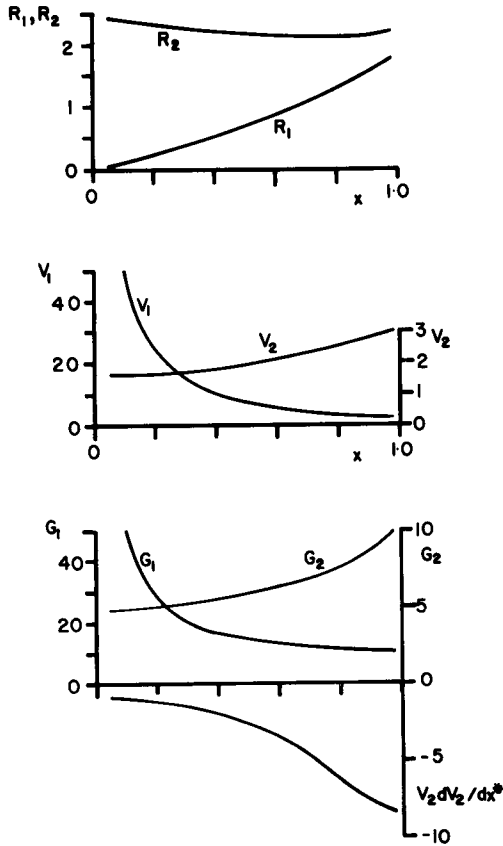
Fig. 3. Results of the model with the second method of evaluating the buoyant body force and with $a = 0.085$, $\gamma = 1.0$, $a_\beta = 0.056$ and $h/r_2 = 2.0$. This run gave $x_{max} = 1.55$.

Fig. 4. Results of the model with the second method of evaluating the buoyant body force and with $a = 0.10$, $\gamma = 1.0$, $a_\beta = 0.056$ and $h/r_2 = 2.0$. This run gave $x_{max} = 1.65$.

a_γ parameterizes the entrainment into the outer plume from the inner plume and as there is no *à priori* reason to assume that $\gamma = 1.0$ (i.e. $a_\gamma = a$) we have run the model with different values of γ. Fig. 5 shows the results with $\gamma = 0.5$ and 1.5 and we see that γ has quite a sensitive effect on the shape of the outer edge of the outer plume near its top.

The fourth parameter we can vary is the size of the cap at the top of the structure. In all the examples above we have used $h/r_2 = 2$ but Fig. 6 shows the case with $h/r_2 = 0$. This change also has a marked effect on the R_2 profile near the top of the plume. With $h/r_2 = 0$, the outer plume is started with a much larger radius and a much smaller velocity. Consequently it accelerates (*i.e.* $V_2 dV_2/ dx^* > 0$) and so it tends to become narrower. This shows why we have chosen $h/r_2 = 2$ as it gives a

"smoother" start to the outer plume, that is, the outer plume does not "neck down" abruptly near the top of the plume and the acceleration also has a smoother variation with height.

The above discussion gives an indication of the sensitivity of the model to variations of a, γ and h/r_2. We do not intend here to juggle all the parameters of the system so as to give the best fit with the observed laboratory flow. To do this would involve having all three entrainment coefficients a function of the height (or the Froude numbers at each height) and would not lead to any new insights into the flow.

The main purpose of this work is however to compare the consequences of the two different buoyant force formulations. Fig. 7 shows the results of the model with the first method of evaluating the buoyant body force and this is to be compared with Fig. 3 which uses the same values of the four parameters a, γ, a_β and h/r_2. This shows that there are some significant differences between the results
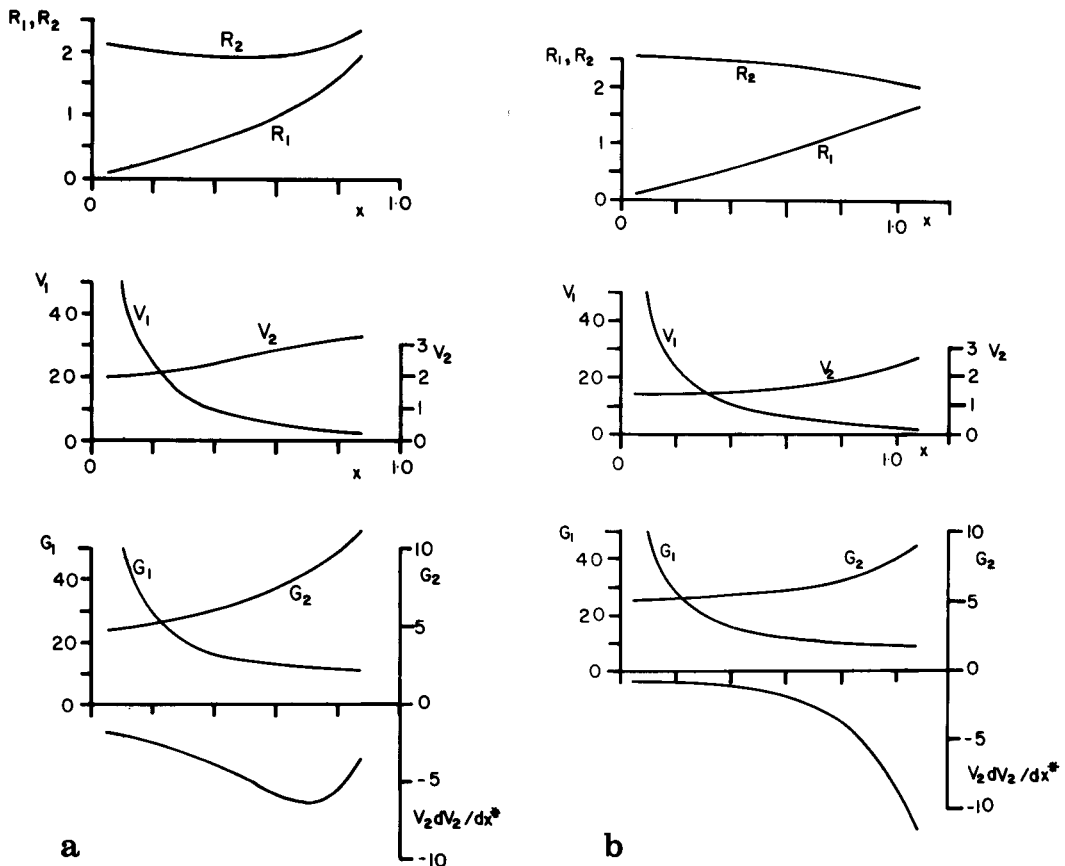
Fig. 5. Results of the model with the second method of evaluating the buoyant body force and with $a = 0.085$, $\gamma = 0.5$ (figure (a)) and $\gamma = 1.5$ (figure (b)), $a_\beta = 0.056$ and $h/r_2 = 2.0$. These runs gave $x_{max} = 1.48$ (figure (a)) and $x_{max} = 1.59$ (figure (b)).

of the two different methods of evaluating the buoyant body forces. With the first method the inner plume expands quite rapidly near the top of its travel and this occurs because the inner plume has a greater downwards buoyant force acting on it. In this case the body force is proportional to $(\rho_1 - \rho_0)$ whereas with the second method of evaluating the body forces the corresponding density difference is only $(\rho_1 - \rho_2)$ but of course there is also the extra factor of the acceleration of the outer plume. In other words, the second method of evaluating the body forces partially shields the inner plume from directly "seeing" the density of the environment and this allows the plume to rise further ($x_{max} = 1.55$ instead of 1.29).

The most important result to arise from this study is the fact that the two different methods of

evaluating the buoyant body forces on the double plume structure do give significantly different results. For example, the maximum non-dimensional height of rise of the structure is 20% higher with the second method than with the first. The previous comparisons between the two methods by McDougall (1978) showed very little difference between the methods but the reasons for this were given in that paper and they arose because the flow being studied was a bubble plume. It is however not possible to say with any degree of confidence which method of buoyant force evaluation corresponds closest with experiment because there are too many arbitrary approximations in the model (e.g. top-hat profiles of properties across the plume) to allow a detailed comparison to be made. Having said this, we note
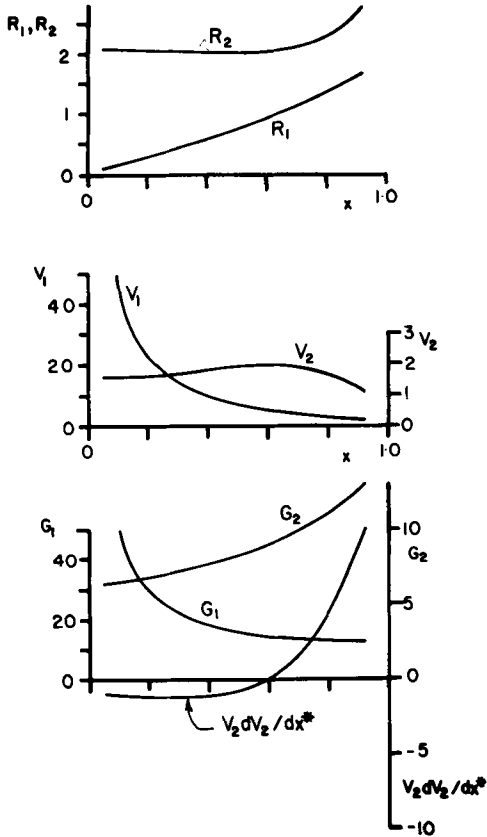
Fig. 6. Results of the model with the second method of evaluating the buoyant body force with $\alpha = 0.085$, $\gamma = 1.0$, $\alpha_\beta = 0.056$ and $h/r_2 = 0$. This run gave $x_{max} = 1.16$.
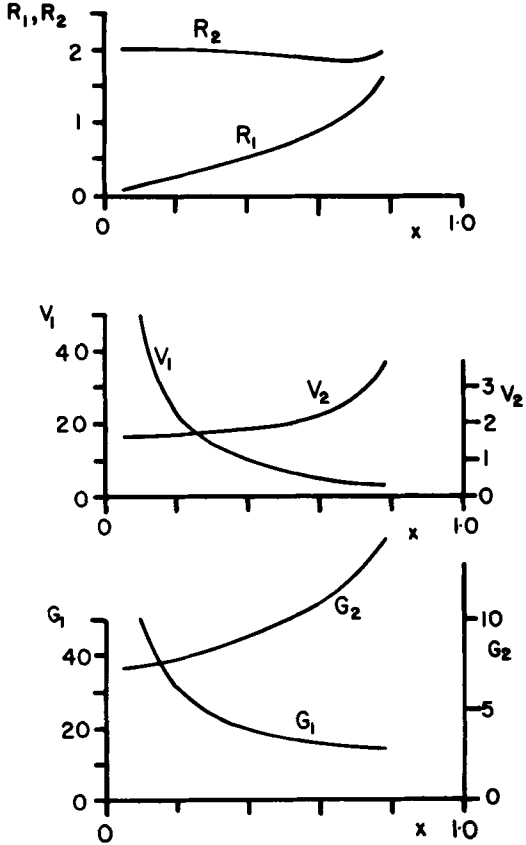
Fig. 7. Results of the model with the first method of evaluating the buoyant body force with $\alpha = 0.085$, $\gamma = 1.0$. $\alpha_\beta = 0.056$ and $h/r_2 = 2.0$. This run gave $x_{max} = 1.29$.

that by using the standard values of $\alpha_\beta = 0.056$ and $\alpha = 0.085$, together with the "best guess" values $\gamma = 1.0$ and $h/r_2 = 2.0$, the second method of evaluating the body force gives $x_{max} = 1.55$ which is closer to the experimental value $x_{max} = 1.50$ than the first method which gives $x_{max} = 1.29$.

Another overall parameter which can be compared between the model and the experiments is the ratio of the height of the plume to its width. Laboratory observations show this ratio to be close to 2.0, but the model of this paper gives much larger values ranging from 3.8 to 4.0. One plausible reason why the computer model seriously under-

estimates the width of the double-plume structure is that the model has top-hat profiles of velocity and density and so the width scale is compressed in relation to the measured outside radius r_2 which reflects the maximum radius attained by *any* plume fluid.

4. Acknowledgements

REFERENCES

Berson, F. A. and Baird, G. 1975. A numerical model of cumulonimbus convection generating a protected core. *Quart. J. Roy. Met. Soc. 101*, 911–928.

List, E. J. and Imberger, J. 1973. Turbulent entrainment in buoyant jets and plumes. *J. Hydraul. Div., Proc. A.S.C.E. 99*, 1461–1474.

McDougall, T. J. 1978. Bubble plumes in stratified environments. *J. Fluid Mech. 85*, 655–672.

Morton, B. R. 1959. Forced Plumes. *J. Fluid Mech. 5*, 151–163.

Morton, B. R. 1962. Coaxial Turbulent jets. *Int. J. Heat Mass Transfer. 5*, 955–965.

Turner, J. S. 1966. Jets and plumes with negative or reversing buoyancy. *J. Fluid Mech. 26*, 779–792.

Turner, J. S. 1973. *Buoyancy Effects in Fluids.* Cambridge University Press.

Turner, J. S. and Gustafson, L. B. 1978. The flow of hot saline solutions from vents in the sea floor—some implications for exhalative massive sulfide and other ore deposits. *Economic Geology. 73*, 1082–1100.